MucosalImmunology

www.nature.com/mi

ARTICLE

ADP/P2Y$_1$ aggravates inflammatory bowel disease through ERK5-mediated NLRP3 inflammasome activation

Chengfei Zhang[1,2], Juliang Qin[1,3], Su Zhang[1], Na Zhang[1], Binhe Tan[1], Stefan Siwko[4], Ying Zhang[1], Qin Wang[3], Jinlian Chen[3], Min Qian[1], Mingyao Liu[1] and Bing Du[1]

Inflammasomes are essential for inflammation and pathogen elimination in response to microbial infection and endogenous danger signals. However, the mechanism of inflammasome activation by endogenous danger signals mediated posttranslational modification and the connection between inflammasomes and inflammatory diseases remains elusive. In this study, we found that ADP was highly released from injured colonic tissue as a danger signal during inflammatory bowel disease. Consequently, extracellular ADP activated the NLRP3 inflammasome through P2Y$_1$ receptor-mediated calcium signaling, which led to the maturation and secretion of IL-1β and further aggravation of experimental colitis. Genetic ablation or pharmacological blockade of the P2Y$_1$ receptor significantly ameliorated DSS-induced colitis and endotoxic shock through reducing NLRP3 inflammasome activation. Moreover, ERK5-mediated tyrosine phosphorylation of ASC was essential for activation of the NLRP3 inflammasome. Thus, our study provides a novel theoretical basis for posttranslational modification of ASC in NLRP3 inflammasome activation and revealed that ADP/P2Y$_1$ is a potential drug target for inflammatory bowel disease.

Mucosal Immunology (2020) 13:931–945; https://doi.org/10.1038/s41385-020-0307-5

INTRODUCTION

The inflammasomes are a class of intracellular protein complexes that regulate the activation of caspase-1 and inflammation, which are essential for the host to counteract assault from pathogens and resolve endogenous danger signals.[1,2] Several inflammasome complexes have been identified, such as the NLRP1, NLRP3, NLRC4, and AIM2 inflammasomes. The NLRP3 inflammasome is one of the most comprehensively characterized inflammasomes and is composed of NLRP3, ASC, and caspase-1. When it senses the proper pathogen-associated molecular patterns or damage-associated molecular patterns (DAMPs), the NLRP3 inflammasome promotes the maturation and release of interleukin-1β (IL-1β) and IL-18, which then initiates inflammatory responses.[2,3] Although the activation of inflammasome has been found tightly regulated by different interacting proteins and/or modifications, the posttranslational modification (PTM) of core pattern-recognition receptors (PRRs) such as NLRP3, NLRC4, pyrin, the adapter ASC, and the effector caspase-1 has been shown to be critical for the regulation of its activation. Whereas, the mechanisms of PTM of these core PRRs still need to be further clarified, especially how PTM is initiated by endogenous danger signals and immune-related signaling pathways.

Ulcerative colitis is a type of inflammatory bowel disease, which is characterized by chronic and relapsing mucosal inflammation limited to the colon. Patients with ulcerative colitis commonly present with abdominal cramping, diarrhea, anemia, and weight loss. Though it presents little threat to life in the short time, its long-lasting duration and high relapse frequency usually bring considerable pain and distress to patients. More seriously, chronic ulcerative colitis patients are at higher risk for the development of colon cancer.[4–6] Because of its complicated pathogenesis, the colitis is difficult to completely cure with currently available clinical drugs, treatment primarily focuses on the maintenance of remission.[7] Thus, it is very important to find out the specific cause and new target for colitis. IL-1β is a proinflammatory cytokine and has reported with high levels in the colon with active lesions. High level IL-1β promotes the activation and functions of dendritic cells, macrophages, and neutrophils.[8,9] Currently, numerous studies have documented that excessive NLRP3 inflammasome-induced IL-1β aggravates colitis and suggested trying novel strategies to prevent colitis through inhibiting NLRP3 inflammasome activity.[10–13]

Traditionally considered as an energy currency, ATP and ADP are crucial for energy metabolism. In recent years, many studies have demonstrated that nucleotides such as ATP, ADP, UTP, and UDP are released from cells during pathogenic microbial infection and tissue injury.[14,15] These extracellular nucleotides function as a danger signal, alerting nearby cells by interacting in an autocrine or paracrine manner with purinergic receptors, which play an important role in the regulation of immune responses.[16] Purinergic signaling activates G-protein-coupled or ligand-gated ion-channel receptors, with many biologic effects only being discovered recently.[15] For example, ATP and UTP were identified as a critical "find-me" cue to promote clearance of apoptotic cells

[1]Changning Maternity and Infant Health Hospital and School of Life Sciences, Shanghai Key Laboratory of Regulatory Biology, East China Normal University, Shanghai 200241, China; [2]Department of Pathology, School of Basic Medical Sciences, Nanjing Medical University, Nanjing 211166, China; [3]Joint Center for Translational Medicine, Fengxian District Central Hospital, No. 6600 Nanfeng Road, Fengxian District, Shanghai 201499, China and [4]Institute of Biosciences and Technology, Department of Molecular and Cellular Medicine, Texas A&M University Health Science Center, Houston, TX 77030, USA
Correspondence: Mingyao Liu (myliu@bio.ecnu.edu.cn) or Bing Du (bdu@bio.ecnu.edu.cn)
These authors contributed equally: Chengfei Zhang, Juliang Qin

Received: 9 June 2019 Revised: 30 April 2020 Accepted: 15 May 2020
Published online: 9 June 2020

or bacteria.[17,18] The ATP released by dying tumor cells triggers NLRP3 inflammasome activation in dendritic cells[19] via P2X$_7$ purinergic receptors mediated K^+ efflux, initiating an immune response against tumors. Whereas, how K^+ efflux induces assembly of the NLRP3 inflammasome remains elusive. Our previous studies also demonstrated that extracellular UDP and ADP are crucial for host defense against viral and bacterial infection through P2 receptor activation.[20–22] Even so, the functions of extracellular nucleotides and their receptors in inflammatory diseases remain poorly understood.

Here, we demonstrate that ADP released from injured colonic tissue during DSS-induced colitis serves as an endogenous DAMP. This extracellular ADP significantly aggravates the progression of colitis through activating the NLRP3 inflammasome in a P2Y$_1$-dependent manner. Most importantly, we demonstrated that a novel calcium and extracellular signal-regulated kinase 5 (ERK5) activate NLRP3 inflammasome through PTM of ASC. Knockout or inhibition of the P2Y$_1$ receptor significantly ameliorated DSS-induced colitis or LPS-induced endotoxic shock through reducing the NLRP3 inflammasome-mediated immune regulation, suggesting that ADP/P2Y$_1$ signaling might be a potential drug target for colitis and other inflammatory diseases.

RESULTS

ADP aggravates DSS-induced colitis

To investigate the potential role of purinergic signaling during colitis, the release of endogenous ATP and ADP in colonic tissues of DSS-administered mice was examined. To our surprise, release of both ATP and especially ADP was dramatically increased from DSS damaged colonic tissues (Fig. 1a). Colonic epithelial cells isolated from DSS-treated mice also have a twofold increase in ADP release (Fig. 1b), supporting that ADP is deliberately secreted by cells as a signaling molecule during colitis. To investigate the biological significance of ADP secretion during colitis, we assessed the pathological features associated with inflammation in mice after treatment with DSS and ADP versus DSS alone. DSS combining with ADP-treated mice suffered from a significant loss of body weight (Fig. 1c), higher disease activity index (DAI) scores (Fig. 1d), and reduced colon length (Fig. 1e), while ADP alone has little influence on mice. In addition, histological analysis of colitis tissue revealed that DSS-treated mice combining with ADP-treated mice have more severe tissue damage, ulceration, and inflammation (Fig. 1f). These results demonstrate that extracellular ADP plays a nonredundant role in exacerbating DSS-induced colitis.

ADP facilitated IL-1β production in inflammatory diseases

To assess the immunological role of ADP in DSS-induced colitis, colonic tissue explants from DSS-treated mice and DSS combining with ADP-treated mice were cultured ex vivo and the secretion of proinflammatory cytokines was analyzed by ELISA. DSS combining with ADP-treated mouse colonic tissue released threefold higher levels of IL-1β, while IL-12p40 levels increased around 50%, IL-6 and TNF-α displayed a trend toward higher release without attaining statistical significance (Fig. 2a). In addition, DSS-treated mice colonic tissue explants stimulated with ADP ex vivo also released much more IL-1β, while IL-6, TNF-α, and IL-12 were little affected (Fig. 2b) suggesting that enhanced IL-1β production from colon tissues may mediate ADP aggravation of DSS-induced colitis. To test this hypothesis, LPS-primed bone marrow-derived macrophages (BMDMs) were stimulated with ADP and proinflammatory cytokine secretion was detected. Importantly, ADP alone was not able to induce IL-1β production, indicating that it is not a complete inflammatory signal, but functions to enhance elements of an inflammatory response to additional stimuli. Among the cytokines examined, only IL-1β production was increased significantly in a concentration-dependent manner in ADP-treated cells, while IL-6 and TNF-α were effectively unchanged (Fig. 2c). Besides, low concentration of ADP also induced IL-1β production although it took a longer time (Fig. S1A). Immunoblotting assays revealed that ADP does not increase the expression of pro-IL-1β but promotes the maturation process (Fig. S1B, C). To rule out the possibility of ADP degradation to AMP affecting IL-1β production, we used apyrase to hydrolyze the extracellular ADP. Accordingly, the ADP-induced IL-1β production was completely blocked by apyrase (Fig. 2d). Moreover, combining LPS-induced endotoxic shock with ADP treatment also promoted the production of IL-1β and led to higher mortality rates (Fig. 2e, f). Taken together, these data suggest that extracellular ADP plays a critical role in promoting IL-1β maturation during inflammatory diseases.

ADP facilitates IL-1β production through activating the NLRP3 inflammasome

To determine whether NLRP3 inflammasome activation mediates ADP's effect on inflammatory cytokines, we initially stimulated LPS-primed BMDMs with ADP and determined the production of IL-18. As shown in Fig. 3a, b, extracellular IL-18 was also increased significantly by ADP in a concentration-dependent manner, which was blocked by hydrolyzing ADP with apyrase. Then LPS-primed NLRP3$^{+/+}$ and NLRP3$^{-/-}$ BMDMs were treated with ADP. Our results revealed that ADP only promoted the production of IL-1β in NLRP3$^{+/+}$ BMDMs, and not in NLRP3$^{-/-}$ BMDMs. However, the NLRP3 inflammasome-independent cytokine TNF-α was not affected by ADP under the same conditions (Fig. 3c). Consistent with these findings, ADP dramatically promoted caspase-1 activation in NLRP3$^{+/+}$ BMDMs, but had little effect on NLRP3$^{-/-}$ BMDMs (Fig. 3d), suggesting that ADP activates the NLRP3 inflammasome. To investigate whether ADP accelerates colitis in a NLRP3 inflammasome-dependent manner, DSS-treated mouse colonic tissue explants were cultured ex vivo and stimulated with ADP. As shown in Fig. 3e, ADP dramatically promoted caspase-1 activation in mouse colonic tissue explants. Furthermore, DSS-administered NLRP3$^{-/-}$ mice were treated with or without ADP. Consistent with our cellular data, ADP-induced aggravation of colitis was eliminated in NLRP3-knockout mice (Fig. 3f–h). Taken together, these results demonstrate that ADP aggravates experimental colitis in a NLRP3 inflammasome-dependent manner.

ADP activates the NLRP3 inflammasome through the P2Y$_1$ receptor

P2Y$_1$, P2Y$_{12}$, and P2Y$_{13}$ are all specific receptors for ADP.[23] To elucidate which receptor is responsible for ADP activated NLRP3 inflammasome, LPS-primed wild-type and P2Y$_1$ deficient BMDMs were stimulated with ADP. Knockout of P2Y$_1$ dramatically suppressed NLRP3 inflammasome-mediated IL-1β and IL-18 production (Fig. 4a), while TNF-α was not affected (Fig. S2A). Accordingly, the increased IL-1β production due to ADP treatment during LPS-induced endotoxic shock was eliminated in P2Y$_1$ deficient mice (Fig. 4b). TNF-α was not affected in either P2Y$_1^{+/+}$ or P2Y$_1^{-/-}$ mice (Fig. S2B). Meanwhile, inhibition of P2Y$_1$ receptor with MRS2179 also suppressed ADP-induced IL-1β production (Fig. 4c). Moreover, P2Y$_1$ receptor deficiency dramatically inhibited NLRP3 inflammasome-mediated caspase-1 activation (Fig. 4d), suggesting that P2Y$_1$ is essential for ADP activation of the NLRP3 inflammasome. In contrast, knockout of P2Y$_{12}$ and P2Y$_{13}$ had a modest effect on ADP-induced IL-1β production (Fig. S2C, D), suggesting that ADP activates the NLRP3 inflammasome primary dependent of P2Y$_1$. As a classic G-protein-coupled receptor (GPCR), P2Y$_1$ couples the GTP-binding protein subunit alpha q (Gαq) and upon activation triggers downstream calcium signaling.[24] To verify whether Gαq is involved in NLRP3 inflammasome activation by ADP, Gαq was silenced by small interfering RNA (siRNA) in BMDMs and we found that knockdown of Gαq obviously inhibited ADP-induced caspase-1 activation (Fig. 4e). Besides, Gαq inhibitor YM-254890 dramatically

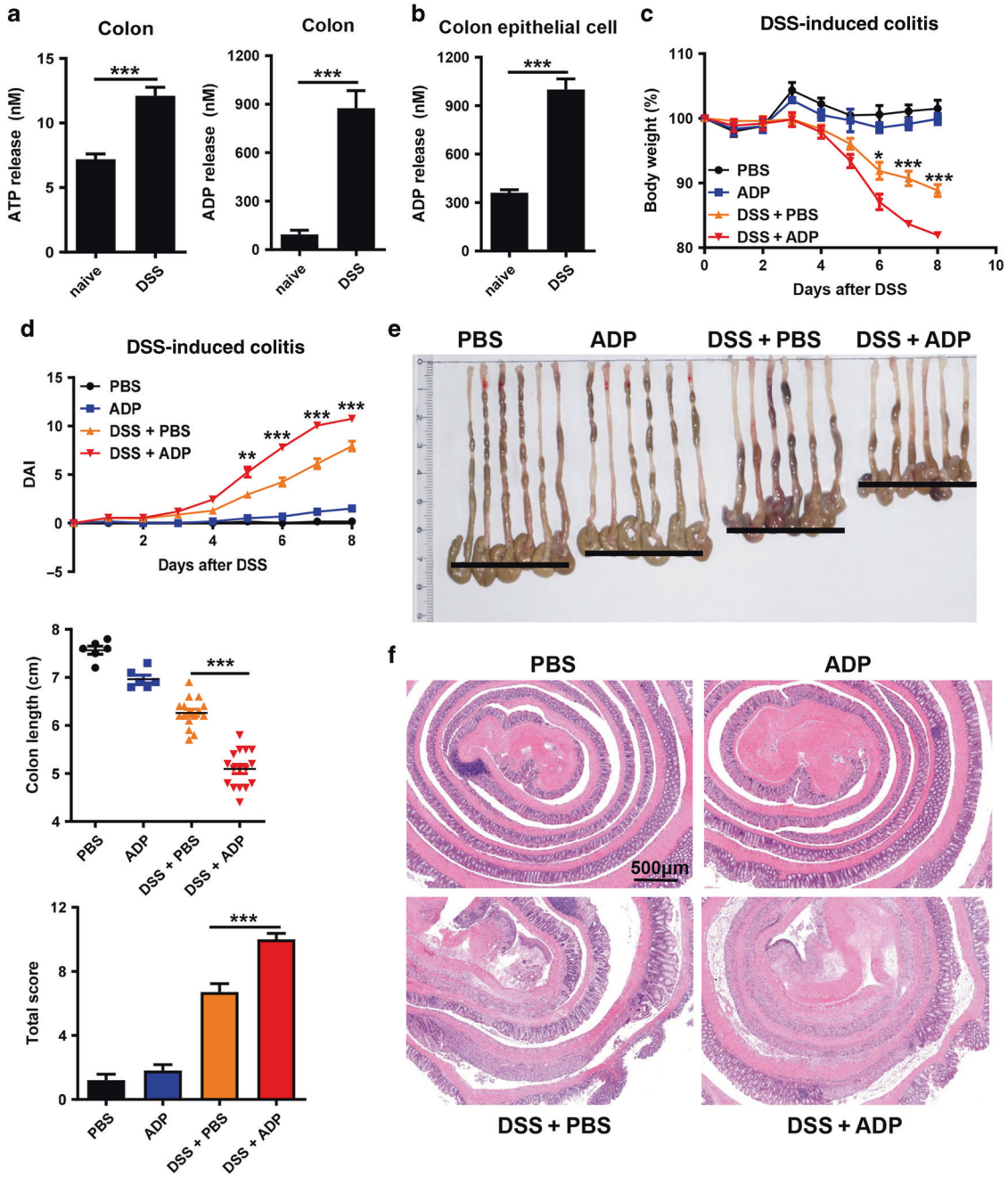

Fig. 1 ADP is a danger signal that aggravates DSS-induced colitis. a WT mice were treated with 2.5% DSS for 7 days, ATP and ADP released from colon fractions were quantified. **b** WT mice were treated with 2.5% DSS for 7 days and colon epithelial cells were isolated, levels of ADP released from colon epithelial cells were quantified. **c**, **d** WT mice were treated with or without 2.5% DSS for 8 days and received PBS or ADP (100 mg/kg) daily by oral gavage from day 1 to day 7. $n = 6$/PBS group, $n = 6$/ADP group, $n = 17$/DSS + PBS group, and $n = 17$/DSS + ADP group. Mouse body weight and disease activity index (DAI) were recorded daily. **e** Mice from **c** were euthanized at day 8, colon lengths were photographed and measured. **f** Histopathology of colon tissues in **c** was examined by H&E staining. Scale bars, 500 μm. Body weight, DAI, and colon length data were pooled analysis from three independent experiments. Pathology score were pooled analysis from two independent experiments. Data are shown as mean ± SEM. *$p < 0.05$; **$p < 0.01$; ***$p < 0.001$.

suppressed the ADP-induced IL-1β release (Fig. 4f). Then, we used U73122 (phospholipase C inhibitor) to block Ca^{2+} mobilization. The ADP-induced IL-1β production and caspase-1 activation were dose dependently decreased by U73122, while the production of TNF-α was not changed (Fig. 4g, h and Fig. S2E). To confirm that, BAPTA-AM was chosen to chelate intracellular Ca^{2+}. As shown in Fig. 4i, BAPTA-AM dose dependently suppressed ADP-induced IL-1β production. In addition, inhibition of Ca^{2+} mobilization by U73122 in DSS-treated mouse colonic tissue explants also eliminated ADP-induced caspase-1 activation (Fig. 4j). Taken together, our results demonstrate that ADP activation of P2Y$_1$ receptor and calcium mobilization is essential for ADP-mediated NLRP3 inflammasome activation.

As the most extensively characterized purinergic receptor to activate NLRP3 inflammasome, we assessed whether P2X7 involved in ADP-mediated NLRP3 inflammasome activation. As shown in Fig. S2F, G, knockout or inhibition of P2X7 had no influence on ADP-induced IL-1β production, suggesting that ADP

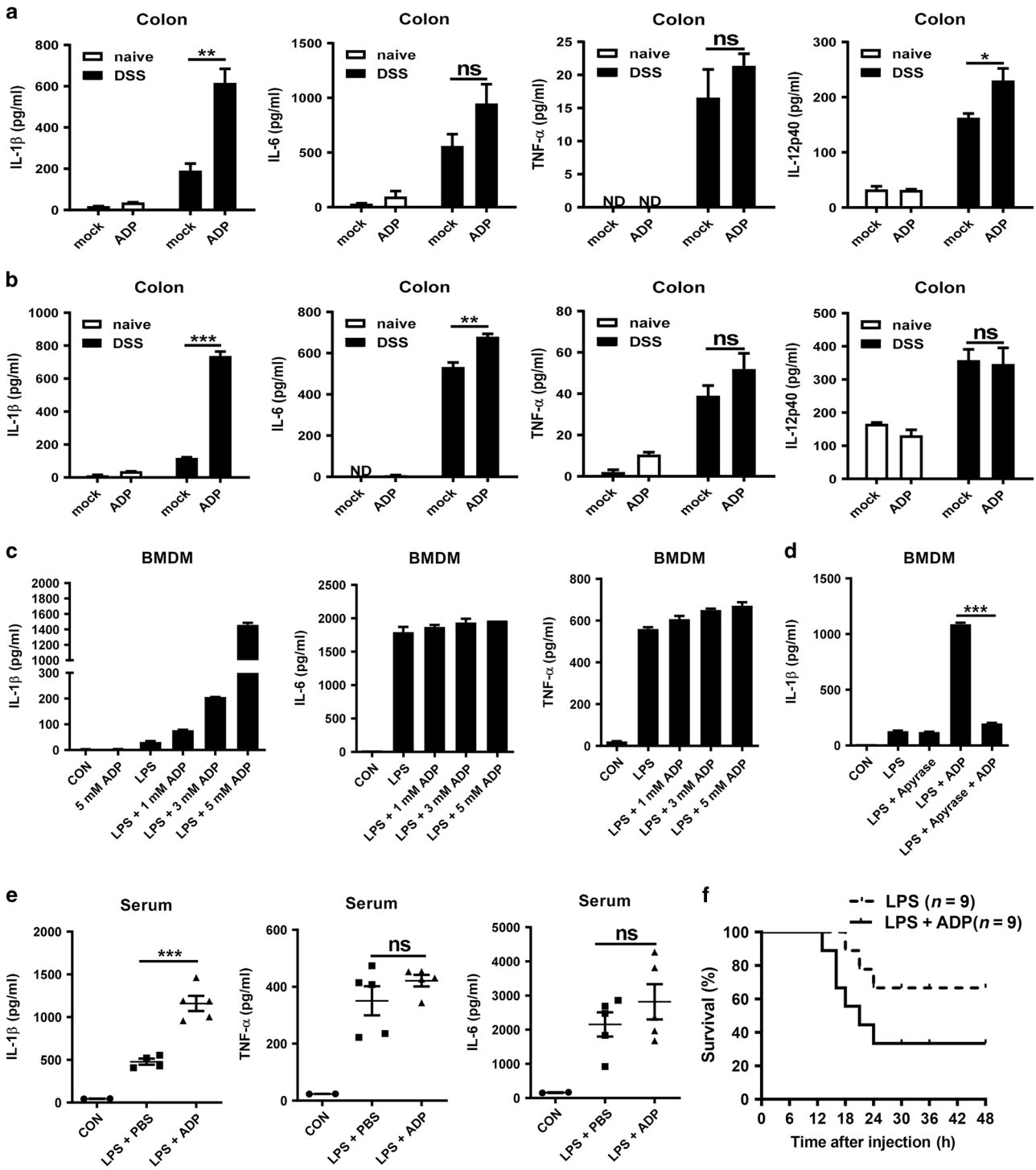

Fig. 2 ADP facilitated colon production of IL-1β. a WT mice were treated with 2.5% DSS for 7 days and received PBS or ADP (100 mg/kg) daily by oral gavage from day 1 to day 7, then the mice were sacrificed and 0.15 g colon sections were cultured in DMEM for 8 h. Secreted proinflammatory cytokines in culture supernatant were measured by ELISA. **b** WT mice were treated with 2.5% DSS for 7 days and euthanized at day 7, 0.15 g colon sections were cultured in DMEM for 6 h and then stimulated with ADP (5 mM) for 2 h. Secreted proinflammatory cytokines in the culture supernatant were measured by ELISA. **c** LPS-primed BMDM cells were stimulated with indicated concentrations of ADP for 1 h, then production of IL-1β, IL-6, and TNF-α was measured by ELISA. **d** LPS-primed BMDM cells were pretreated with 1 U/ml apyrase or not for 1 h and then stimulated with ADP (5 mM) for 1 h. Production of IL-1β was measured by ELISA. **e** 6-week-old mice were intraperitoneally primed with LPS (20 mg/kg) for 6 h and then intraperitoneally challenged with ADP (300 mg/kg) for 1 h. Production of IL-1β, IL-6, and TNF-α in mouse serum was measured by ELISA. **f** 6-week-old mice were treated as in **e** and the survival of mice was recorded for 48 h. Data are shown as mean ± SEM. *$p < 0.05$; **$p < 0.01$; ***$p < 0.001$; ns not significant, ND not detected.

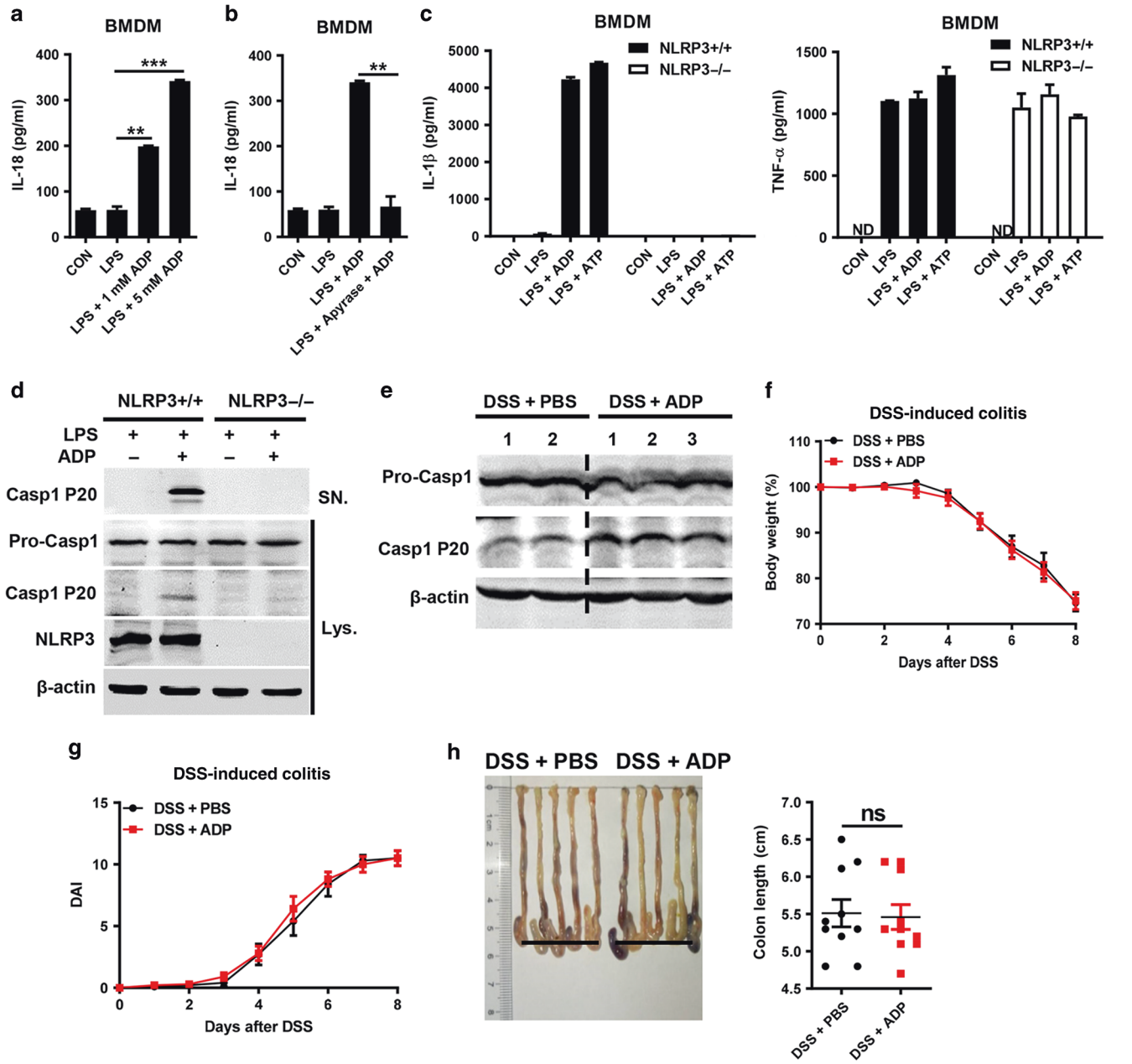

Fig. 3 ADP facilitated the production of IL-1β through activating the NLRP3 inflammasome. a LPS-primed BMDM cells were stimulated with indicated concentrations of ADP for 1 h, and production of IL-18 was measured by ELISA. **b** LPS-primed BMDM cells were pretreated with 1 U/ml apyrase or not for 1 h and then stimulated with ADP (5 mM) for 1 h, production of IL-18 was measured by ELISA. **c** LPS-primed NLRP3$^{+/+}$ and NLRP3$^{-/-}$ BMDM cells were stimulated with ADP (5 mM) or ATP (5 mM) for 1 h, and production of IL-1β and TNF-α were measured by ELISA. **d** LPS-primed NLRP3$^{+/+}$ and NLRP3$^{-/-}$ BMDM cells were stimulated with 5 mM ADP for 80 min. Cleaved caspase-1 (p20) in culture supernatants (SN) or in cell lysates (Lys), as well as the precursor of caspase-1 (pro-caspase-1) and NLRP3 in cell lysates were assessed by immunoblotting. **e** 8-week-old mice were treated with 2.5% DSS for 7 days and euthanized at day 7, 0.15 g colon fractions were cultured in DMEM for 6 h and then stimulated with ADP (5 mM) for 2 h. Pro-caspase-1 and cleaved caspase-1 (p20) in colon lysates were assessed by immunoblotting. Each lane represents a sample from an individual mouse. **f**, **g** NLRP3$^{-/-}$ mice were treated with 2.5% DSS for 8 days and received PBS or (100 mg/kg) ADP daily by oral gavage from day 1 to day 7. Mouse body weight and disease activity index (DAI) were recorded daily. $n = 10$ per group. **h** Mice from **f** were sacrificed at day 8 and the colon lengths were recorded. Body weight, DAI, and colon length data were pooled analysis from two independent experiments. Data are shown as mean ± SEM. $^{**}p < 0.01$; $^{***}p < 0.001$; ns not significant, ND not detected.

activates the NLRP3 inflammasome independent of P2X7. A previous study reported that ADP can be synthesized into ATP by ecto-adenylate kinase.[25] To evaluate whether ADP-induced IL-1β production due to extracellular ATP generated by ecto-adenylate kinase, LPS-primed wild-type and P2Y$_1$ deficient BMDMs were stimulated with ATP. We found that ATP-induced IL-1β production was not affected in wild-type and P2Y$_1$ deficient BMDMs (Fig. S2H). Similarly, inhibition of P2Y$_1$ receptor with MRS2179 also had no influence on ATP-induced IL-1β production (Fig. S2I). Considering knockout or inhibition of P2Y$_1$ dramatically suppressed ADP-triggered IL-1β production, we thought ADP activates the NLRP3 inflammasome independent of extracellular ATP generated by ecto-adenylate kinase. K^+ efflux is essential for many stimuli to activate the NLRP3 inflammasome. To investigate the potential

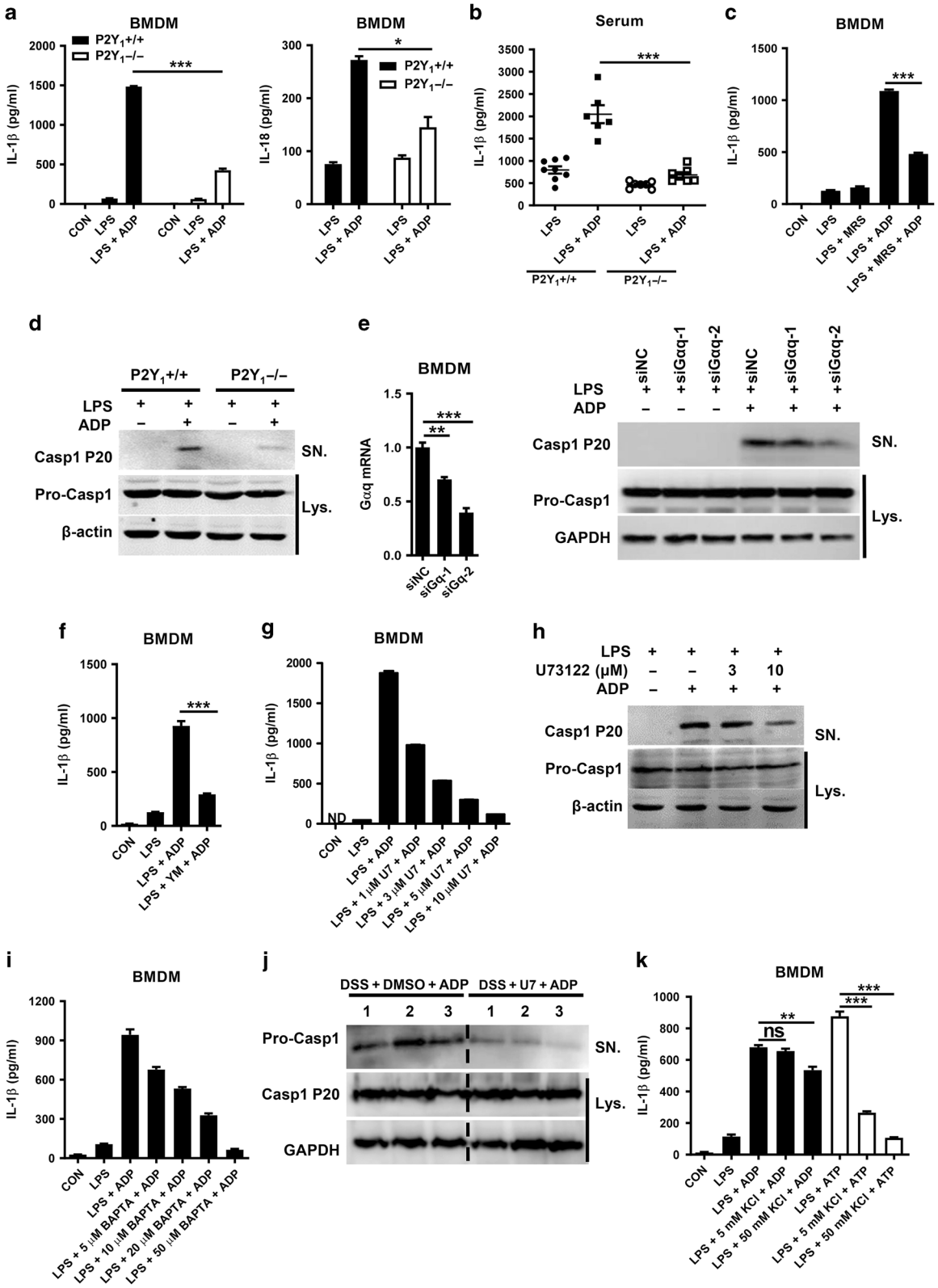

role of K^+ efflux during ADP activates the NLRP3 inflammasome, we used medium containing high KCl to prevent K^+ efflux. As shown in Fig. 4k, the presence of high KCl dramatically inhibited ATP-triggered (requirement for decreased cytosolic K^+ in NLRP3 activation) IL-1β release but slightly decreased ADP-triggered IL-1β release, suggesting that ADP can activates NLRP3 inflammasome independent of K^+ efflux. Taken together, these data suggest that ADP activates the NLRP3 inflammasome independent of P2X7, ecto-adenylate kinase, and K^+ efflux. ADP and ATP have different ways to activate NLRP3 inflammasome.

Fig. 4 ADP activates the NLRP3 inflammasome through P2Y$_1$ and the calcium pathway. a LPS-primed P2Y$_1^{+/+}$ and P2Y$_1^{-/-}$ BMDM cells were treated with ADP (5 mM) for 1 h and production of IL-1β and IL-18 were measured by ELISA. **b** P2Y$_1^{+/+}$ and P2Y$_1^{-/-}$ mice were intraperitoneally treated with 20 mg/kg LPS for 6 h and then intraperitoneally challenged with ADP (300 mg/kg) for 1 h, production of IL-1β in serum was measured by ELISA. **c** LPS-primed BMDM cells were pretreated or not with MRS2179 (10 μM) for 1 h and then stimulated with ADP (5 mM) for 1 h, production of IL-1β was detected by ELISA. **d** LPS-primed P2Y$_1^{+/+}$ and P2Y$_1^{-/-}$ PEM cells were stimulated with ADP (5 mM) for 80 min, then levels of cleaved caspase-1 (p20) in culture supernatants (SN) and pro-caspase-1 in cell lysates were assessed by immunoblotting. **e** BMDM cells were transfected with negative control siRNA or Gαq-specific siRNA for 72 h (48 h for Gαq mRNA detection) and then primed with LPS (500 ng/ml) for 6 h. The cells were then treated with ADP (5 mM) for 80 min, cleaved caspase-1 (p20) in culture supernatants (SN) and pro-caspase-1 in cell lysates were assessed by immunoblotting. **f** LPS-primed BMDM cells were pretreated with 1 μM YM-254890 for 1 h and then stimulated with ADP (5 mM) for 1 h, production of IL-1β was measured by ELISA. **g** LPS-primed BMDM cells were pretreated with indicated concentrations of U73122 for 1 h and then stimulated with ADP (5 mM) for 1 h, production of IL-1β was measured by ELISA. **h** LPS-primed BMDM cells were pretreated with 3 or 10 μM U73122 for 1 h and then stimulated with ADP (5 mM) for 80 min, cleaved caspase-1 (p20) in culture supernatants (SN) and pro-caspase-1 in cell lysates were assessed by immunoblotting. **i** LPS-primed BMDM cells were pretreated with indicated concentrations of BAPTA-AM for 1 h and then stimulated with ADP (5 mM) for 1 h, production of IL-1β was measured by ELISA. **j** 8-week-old mice were treated with 2.5% DSS for 7 days and euthanized at day 7, 0.15 g colon fractions were cultured in DMEM with or without 10 μM U73122 for 6 h and then stimulated with ADP (5 mM) for 2 h. Cleaved caspase-1 (p20) in culture supernatants (SN) and pro-caspase-1 in colon lysates were assessed by immunoblotting. Each lane represents a sample from an individual mouse. **k** LPS-primed BMDM cells were treated with KCl (5 and 50 mM) and ADP (5 mM) or ATP (5 mM) for 1 h, production of IL-1β was detected by ELISA. Data are shown as mean ± SEM. $*p < 0.05$; $**p < 0.01$; $***p < 0.001$; ns not significant, ND not detected.

P2Y$_1$ receptor deficiency ameliorates DSS-induced colitis

To evaluate the role of the P2Y$_1$ receptor during colitis, P2Y$_1^{+/+}$ and P2Y$_1^{-/-}$ mice were treated with DSS. Body weight loss, colon length reduction, and tissue damage were all significantly alleviated in P2Y$_1$ deficiency mice (Fig. 5a–c). Furthermore, the production of IL-1β from P2Y$_1$-deficiency colonic tissue explants was reduced, while IL-6 was little changed (Fig. 5d). In addition, the survival of P2Y$_1$-deficiency mice was also much higher than WT mice (Fig. 5e), suggesting that ADP aggravates DSS-induced colitis in a P2Y$_1$-dependent manner. Next, we treated DSS-treated mice with the P2Y$_1$ inhibitor MRS2179 and found that the clinical features of colitis such as weight loss, DAI, and colon length reduction were all attenuated by MRS2179 (Fig. 5f–h). Meanwhile, the production of IL-1β from MRS2179-treated colonic tissue explants was also reduced, whereas IL-6, TNF-α, and IL-12 were reduced to a lesser extent or unchanged (Fig. 5i). Thus, these data indicate that blocking the P2Y$_1$ receptor significantly ameliorates DSS-induced mouse colitis, implying that ADP/P2Y$_1$ signaling might be a potential drug target for colitis.

ERK5 is essential for ADP to activate the NLRP3 inflammasome

Although previous data have shown that calcium mobilization is essential for NLRP3 inflammasome activation, the molecular pathways directly involved in calcium mediated inflammasome activation are uncertain.[26] Thus, we analyzed gene expression changes in LPS-primed macrophages treated with or without ADP by microarray and the genes whose expression changed more than 20-fold were selected and analyzed by KEGG database or analyzed in refs. [27–29] We found that half of the dozen most highly increased genes were correlated with ERK5, which is a downstream target of calcium signaling. Consequently, when we inhibited calcium mobilization or ERK5 with 2-APB or XMD8-92, respectively, the elevated expression of these genes was blocked (Fig. S3A, B). Chelating intracellular Ca^{2+} by BAPTA-AM also suppressed the expression of ADP-induced genes (Fig. S3C). Moreover, ADP dramatically promoted ERK5 phosphorylation and this activation could be prevented by chelating intracellular Ca^{2+} (Fig. 6a, b). Furthermore, we pretreated LPS-primed BMDM with the ERK5 inhibitor XMD8-92 before ADP activation to explore the function of ERK5 in NLRP3 inflammasome activation. As shown in Fig. 6c, d and Fig. S4A, XMD8-92 dramatically suppressed NLRP3 inflammasome-dependent IL-1β production. However, the production of TNF-α and the expression of pro-IL-1β was not significantly affected. Accordingly, LPS-induced IL-1β production was significantly inhibited by XMD8-92 in WT mice but not in NLRP3-knockout mice (Fig. 6e and Fig. S4B). Again, TNF-α production was not changed (Fig. S4C). Similarly, ERK5 knockdown by siRNA in BMDMs significantly inhibited ADP-induced IL-1β secretion but did not affect the secretion of TNF-α (Fig. 6f and Fig. S4D, E). Similarly, caspase-1 cleavage was also reduced in ERK5-knockdown BMDMs (Fig. 6g). To confirm the function of ERK5 in NLRP3 inflammasome activation, an ERK5-knockout HEK293T cell line was generated. Then, we exogenously expressed components of the NLRP3 inflammasome system in WT and ERK5-knockout HEK293T cells. As shown in Fig. 6h, ERK5-knockout cells showed reduced IL-1β secretion compared with that in WT HEK293T cells. Then we re-expressed ERK5 in ERK5-knockout HEK293T cells and found that the secretion of IL-1β was restored (Fig. 6i). The formation of ASC specks is considered a classical marker for inflammasome activation.[30] Consistent with previous reports, stimulation of LPS-primed BMDM with ADP induced the formation of ASC specks, but this was greatly reduced by the ERK5 inhibitor XMD8-92 (Fig. 6j). Moreover, inhibition of ERK5 in DSS-treated mouse colonic tissue explants also reduced the production of IL-1β (Fig. 6k). Thus, these results support the conclusion that ERK5 is essential for ADP-mediated NLRP3 inflammasome activation. To further explore whether the role of ERK5 is universal in NLRP3 inflammasome activation, we treated the cells with different NLRP3 agonists. These data showed that inhibition or knockdown of ERK5 suppressed ATP, MSU, and alum-induced IL-1β secretion (Fig. S4F, G), suggesting that ERK5 is essential for NLRP3 inflammasome activation.

ERK5 interacts with NLRP3/ASC and regulates ASC phosphorylation

To further elucidate how ERK5 regulates NLRP3 inflammasome activation, we examined whether ERK5 could interact with the components of the NLRP3 inflammasome. As shown in Fig. 7a–c, ERK5 interacted with both NLRP3 and ASC in the presence or absence of LPS or ADP. The NLRP3 inflammasome is released as a particulate danger signal after activation of the inflammasome.[31] However, we found that when treated with both LPS and ADP, macrophages secreted not only NLRP3 inflammasome components, but also ERK5 (Fig. S5A). These results suggested that ERK5 constitutively physically interacts with NLRP3 or ASC to regulate NLRP3 inflammasome activation. Similarly, using Phos-tag we found that ADP dramatically induced ASC phosphorylation in a time-dependent manner (Fig. 7d). However, the phosphorylation of ASC was reduced obviously in cells with ERK5 deletion or inhibition (Fig. 7e and Fig. S5B). Moreover, ASC in the Triton X-100-insoluble fraction was decreased in ERK5-knockout cells (Fig. 7f). Re-expression of ERK5 restored ASC distribution into the Triton X-100-insoluble fraction in ERK5$^{-/-}$ cells (Fig. 7g) and deletion of ERK5 kinase domain could not restored the production of IL-1β in ERK5-deficient HEK293T cells (Fig. S5C). Previous studies have demonstrated that phosphorylation of human ASC on tyrosine

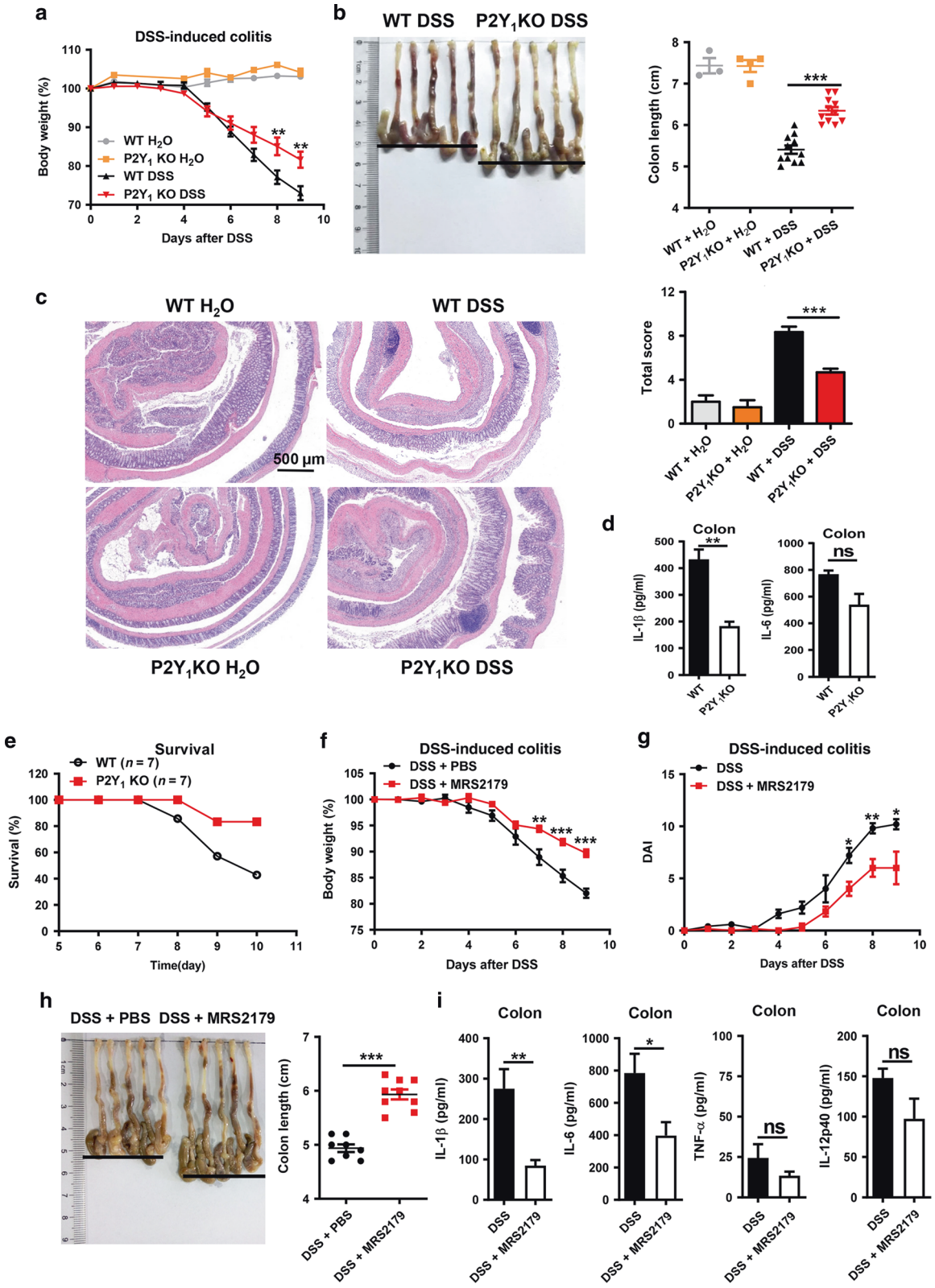

146 is required for inflammasome activation.[32,33] When we expressed a mutant form of ASC, ASC-Y146F, in 293T cells together with ERK5 and NLRP3 inflammasome components, it ablated NLRP3 activation (as measured by translocation to the Triton-insoluble fraction) and the induction of IL-1β production as expected, indicating that ERK5-dependent inflammasome activation proceeds through ASC tyrosine phosphorylation on Y146. However, when inflammasome components were expressed in cells lacking ERK5, there was no change in IL-1β production, further supporting a requirement for ERK5 signaling to activate NLRP3 inflammasome (Fig. 7h and Fig. S5D). As a serine/threonine kinase, ERK5 could not phosphorylate ASC-Y146 directly, so we

Fig. 5 P2Y$_1$ deficiency attenuates DSS-induced colitis. a WT and P2Y$_1^{-/-}$ mice (co-housed together from born to experiments) were treated with 2% DSS or not for 9 days. Body weight changes were recorded daily. $n = 3$/WT + H_2O group, $n = 4$/P2Y$_1^{-/-}$ + H_2O group, $n = 13$/WT + DSS group, and $n = 11$/ P2Y$_1^{-/-}$ + DSS group. **b**, **c** Mice from **a** were euthanized at day 9, colon lengths were measured, and histopathology of colon tissues was examined by H&E staining. Scale bars, 500 μm. Body weight, colon length, and pathology score were pooled analysis from two independent experiments. **d** P2Y$_1^{+/+}$ and P2Y$_1^{-/-}$ mice were treated with 2% DSS for 9 days, then the mice were sacrificed and 0.15 g colon fractions were cultured in DMEM for 8 h. Secreted proinflammatory cytokines IL-1β and IL-6 in the culture supernatant were measured by ELISA. **e** P2Y$_1^{+/+}$ and P2Y$_1^{-/-}$ mice were treated with 2% DSS for 10 days and mouse survival was recorded. **f**, **g** 8-week-old mice were treated with 2.5% DSS for 9 days and received PBS ($n = 8$) or MRS2179 (5 mg/kg, $n = 9$) by oral gavage at day 1, day 3, day 5, and day 7. The body weight and DAI of mice were recorded daily. **h** Mice from **f** were sacrificed at day 9 and the colon lengths were recorded. Body weight and colon length were pooled analysis from two independent experiments. **i** 0.15 g colon sections from **f** were cultured in DMEM for 8 h. Secreted proinflammatory cytokines in the culture supernatant were measured by ELISA. Data are shown as mean ± SEM. *$p < 0.05$; **$p < 0.01$; ***$p < 0.001$; ns not significant.

speculated there may be other kinases mediated this process. SYK, PYK2 and BTK are well defined tyrosine kinase to drive the phosphorylation of ASC-Y146.[32–34] To verify whether these tyrosine kinases mediate the ability of ERK5 to drive the phosphorylation of ASC-Y146, LPS-primed BMDMs were pre-treated with ERK5 inhibitor XMD8-92 before ADP stimulation and then the phosphorylation of SYK, PYK2 and BTK were analyzed by immunoblotting. As shown in Fig. 7i, we found that ADP dramatically promoted the phosphorylation of PYK2 and ERK5 inhibitor XMD8-92 dramatically suppressed this process, while the phosphorylation of SYK and BTK were little changed. Furthermore, ASC in the Triton X-100-insoluble fraction, ADP-triggered IL-1β release, and caspase-1 activation were all decreased obviously by PYK2 inhibitor (Fig. 7j, k and Fig. S5E). In summary, these results demonstrate that ERK5 regulated tyrosine phosphorylation of ASC is essential for the activation of the NLRP3 inflammasome. PYK2 is the tyrosine kinase that mediates the ability of ERK5 to drive phosphorylation of ASC-Y146.

DISCUSSION

The gastrointestinal environment is a complicated system that contains with the majority of the immune cells in the body and more than ten trillion microorganisms separated by a layer of mucus and a layer of epithelial cells. Once the physical barrier is broken, the invading pathogens may trigger an unrestrained immune response that underlies inflammatory bowel diseases (IBD). The gastrointestinal innate immune system contributes to IBD pathology through sensing host-derived cellular stress signals or pathogenic microbes by PRRs.[35] Apart from PRRs, purinergic receptors are implicated in the pathogenesis of gastrointestinal disorders and are being investigated as potential therapeutic targets. Among these purinoceptors, P2X7 and its endogenous ligand ATP play important roles in both the initiation and exacerbation of intestinal inflammation.[36] Furthermore, secretion of ATP by infected or injured macrophages leads to NLRP3 inflammasome activation via activation of the P2X7 receptor.[37] Interestingly, we observed a much higher release of ADP (~800 nM) in both DSS damaged colon tissues and epithelial cells when compared with ATP (~12 nM). However, the function of ADP and its purinoceptors in both inflammasome activation and inflammatory bowel disease has been poorly investigated. In this study, we demonstrated that ADP is a DAMP that significantly aggravates DSS-induced colitis through activating the NLRP3 inflammasome in a calcium- and ERK5-dependent manner, which provides new insight into the activation and regulation mechanisms of the NLRP3 inflammasome at physiological levels of posttranscriptional modification. Therefore, our data suggest that therapeutic interventions that target ADP and its receptors may show clinical benefit for the treatment of IBD.

In the past few years, various GPCRs have been reported to activate and regulate the NLRP3 inflammasome by sensing multiple ions, metabolites, and neurotransmitters, suggesting that GPCR signaling is an important regulator of the NLRP3 inflammasome. However, the GPCRs are widely distributed and the activation of these GPCRs may induce multiple effects depending on the tissue where they are expressed and the signaling cascades that they induce.[38] Although P2Y$_1$, P2Y$_{12}$, and P2Y$_{13}$ are all GPCRs that bind ADP, the downstream signaling pathways are different. Activation of P2Y$_1$ evokes calcium mobilization via the Gαq. In contrast, P2Y$_{12}$ and P2Y$_{13}$ suppress the activity of adenylate cyclase and the production of cAMP through the GTP-binding protein subunit alpha i.[39,40] Both calcium mobilization and cAMP are crucial for regulating NLRP3 inflammasome activity.[26,41,42] In this study, we found that inhibition or knockout of P2Y$_1$ significantly decreased ADP-mediated IL-1β production, while knockout of P2Y$_{12}$ and P2Y$_{13}$ only had marginal influence on NLRP3 inflammasome activation. Thus, we believe that ADP activates the NLRP3 inflammasome mainly through the P2Y$_1$ receptor and calcium signaling. Furthermore, we found that knockout or pharmacological blockade of the P2Y$_1$ receptor significantly ameliorated DSS-induced mouse colitis, which supports the P2Y$_1$ receptor as a potential target for the treatment of colitis.

In this study, we demonstrated that although 30 μM ADP increase the release of mature IL-1β a little in 3 h, the millimolar ADP is perfect for activation of NLRP3 inflammasome even in 1 h. Not only ADP, but also ATP as a classic NLRP3 inflammasome activator has to activate NLRP3 inflammasome in millimolar level. So we speculate that maybe the nucleoside triphosphate diphosphohydrolase 1 (NTPDase1/CD39) will hydrolyze the extracellular ADP to eliminate the function of them.[43,44] Most importantly, the activation of inflammasome is harmful to the normal tissues that triggers cell programmed death called pyroptosis, then causes septic shock and other immunological diseases.[45] Thus, the activation of NLRP3 inflammasome should be tightly controlled in physiological conditions. So the high concentration of ADP/ATP for inflammasome activation could be regard as a kind of protection to the normal tissues.

It has been well established that calcium mobilization activates the NLRP3 inflammasome.[26,46] However, the precise mechanism of calcium mobilization leading to inflammasome activation at the molecular level has been poorly described to date.[47] Thus, we performed a microarray analysis to explore which genes or signal transduction pathways may be involved in ADP-mediated NLRP3 inflammasome activation. Our results suggested that ERK5 is essential for the activation of the NLRP3 inflammasome. ERK5, also termed big mitogen-activated protein kinase-1, is the most recently identified member of the mitogen-activated protein kinase (MAPK) family.[48] While the majority of research efforts have focused on the ERK1/2, JNK, and P38 family members, emerging evidence has now demonstrated an important role for less well-known MAPK family members such as ERK5. While the catalytic core of ERK5 is situated in the N-terminal half, ERK5 displays several distinct structural and functional properties that set it apart from ERK1/2 and the other members of the MAPK family. As the upstream regulator to ERK5, Gαq coupled with lot of GPCRs and play very important

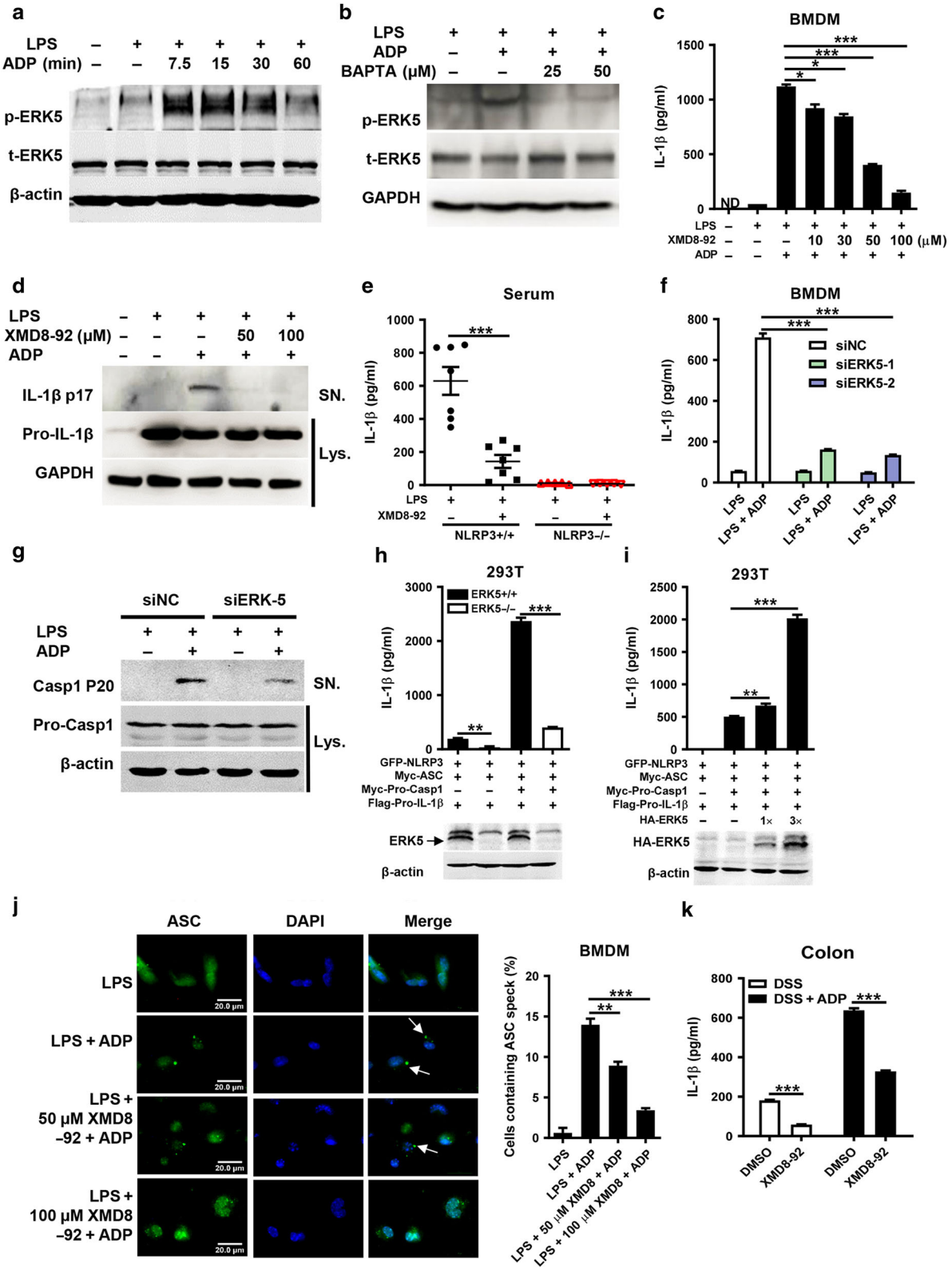

roles in regulation of immune responses. Although the calcium-sensing receptor that also coupled with Gαq has been found to play key roles in activating the NLRP3 inflammasome, we have no idea whether Gαq coupled GPCRs are all involved in inflammasome activation.[26] Actually, till to now, at least 800 GPCRs have been identified from human that only coupled with several kinds of G proteins.[49] It is a very big scientific question that why so many receptors with various functions have the similar or the same coupled G protein. We speculated that the functions of different receptors may be spatially and temporally controlled and great efforts need to be made to explore the regulatory mechanisms of GPCRs. But for this study, we have

Fig. 6 ERK5 is essential for ADP to activate the NLRP3 inflammasome. a LPS-primed BMDM cells were stimulated with ADP (5 mM) for the indicated times, and phosphorylated ERK5 (T218/T220) and total ERK5 were analyzed by immunoblotting. **b** LPS-primed BMDM cells were pretreated with the indicated concentrations of BAPTA-AM for 1 h and then stimulated with ADP (5 mM) for 15 min. ERK5 phosphorylation was analyzed by immunoblotting. **c** LPS-primed BMDM cells were pretreated with indicated concentrations of XMD8-92 for 1 h and then stimulated with ADP (5 mM) for 1 h, production of IL-1β was detected by ELISA. **d** LPS-primed BMDM cells were pretreated with 50 or 100 μM XMD8-92 for 1 h and then stimulated with ADP (5 mM) for 80 min. The expression of pro-IL-1β in cell lysates and mature IL-1β in culture supernatants (SN) were analyzed by immunoblotting. **e** NLRP3$^{+/+}$ and NLRP3$^{-/-}$ mice were intraperitoneally treated with XMD8-92 (50 mg/kg) and LPS (20 mg/kg) for 6 h, and production of IL-1β in serum was measured by ELISA. **f** BMDM cells were transfected with negative control siRNA or ERK5-specific siRNA for 36 h and then primed with LPS (500 ng/ml) for 6 h. The cells were then treated with ADP (5 mM) for 1 h, and production of IL-1β was detected by ELISA. **g** BMDM cells were treated as in **f** and cleaved caspase-1 (p20) in culture supernatants (SN), as well as pro-caspase-1 in cell lysates, were assessed by immunoblotting. **h** The NLRP3 inflammasome was reconstituted in ERK5$^{+/+}$ and ERK5$^{-/-}$ 293T cells by transfection of GFP-NLRP3, Myc-ASC, Myc-pro-caspase-1, and Flag-Pro-IL-1β for 30 h and production of IL-1β was detected by ELISA; expression of ERK5 was assessed by immunoblotting. **i** The NLRP3 inflammasome was reconstituted in ERK5$^{-/-}$ 293T cells by transfection of HA-ERK5, GFP-NLRP3, Myc-ASC, Myc-Pro-caspase-1, and Flag-Pro-IL-1β for 30 h and the production of IL-1β was detected by ELISA; expression of ERK5 was assessed by immunoblotting with HA antibody. **j** LPS-primed BMDMs were treated with XMD8-92 for 1 h and then stimulated with ADP (5 mM) for 1 h. ASC speck formation was detected by immunofluorescence. Scale bars, 20 μm. **k** 8-week-old mice were treated with 2.5% DSS for 7 days and euthanized at day 7, 0.15 g colon fractions were cultured in DMEM with or without XMD8-92 (100 μM) for 6 h and then stimulated with ADP (5 mM) for 2 h. Production of IL-1β was detected by ELISA. Data are shown as mean ± SEM. *p < 0.05; **p < 0.01; ***p < 0.001; ND not detected.

shown solid data that both P2Y$_1$ and Gαq are involved in ADP-mediated NLRP3 inflammasome activation.

The phosphorylation of different inflammasome components plays contradictory roles in the regulation of NLRP3 inflammasomes. PKA induces NLRP3 phosphorylation on Ser 291 to inhibit NLRP3 inflammasome activation in bile acid-controlled inflammation.[50] Whereas, MAPK8 and MAPK9 have been demonstrated to regulate the phosphorylation of the adapter ASC to control inflammasome activity, and phosphorylated ASC can be detected in the Triton X-100-insoluble fraction,[34] indicating inflammasome activation. In this study, we demonstrated that ADP-induced ERK5 kinase activity is necessary for ASC phosphorylation at Y146, which could be the main reason for NLRP3 inflammasome activation. Most importantly, ADP as well as ATP, MSU, and ALUM all activate the NLRP3 inflammasome in an ERK5-dependent manner suggesting that ERK5-mediated ASC phosphorylation is indispensable for NLRP3 inflammasome.

In summary, we demonstrate here that ADP and P2Y$_1$ play a critical role in DSS-induced colitis and LPS-induced endotoxic shock through activating the NLRP3 inflammasome. We also showed that calcium mobilization and ERK5-mediated ASC phosphorylation is a major event that controls inflammasome activation. Thus, it will be of interest to assess whether pharmacological inhibition of the P2Y$_1$-calcium-ERK5 pathway confers protection in systemic inflammatory diseases.

METHODS

Mice

P2Y$_1$$^{-/-}$, P2Y$_{13}$$^{-/-}$, P2X7$^{-/-}$, and NLRP3$^{-/-}$ mice were generated by the CRISPR/Cas system as described previously.[21,51] P2Y$_{12}$$^{-/-}$ mice were a kind gift from Prof. Junling Liu (Shanghai Jiaotong University).[52] All mice were in a C57BL/6 background. C57BL/6 wild-type mice were purchased from the Shanghai Laboratory Animal Company (Shanghai, China). All mice were housed in specific pathogen-free facilities at the Animal Center of East China Normal University. All animal experiments complied with institutional guidelines.

Reagents

ADP, ATP, Apyrase, ATP bioluminescence assay kit, MRS2179, o-ATP, A-740003, A-438079, and KCl were purchased from Sigma. DSS (molecular weight, 36,000–50,000) was obtained from MP Biomedicals. ADP-Glo™ Kinase Assay Kit was purchased from Promega. U73122 and 2-APB were purchased from Tocris. XMD8-92 was purchased from Santa Cruz Biotechnology. YM-254890, BAPTA-AM, and PF-431396 were purchased from MedChemExpress. MSU and ALUM were obtained from Invivogen. Anti-mouse caspase-1 (AG-20B-0042) and anti-NLRP3 (AG-20B-0014) antibodies were purchased from AdipoGen. Anti-ASC (sc-22514) antibody was purchased from Santa Cruz Biotechnology. The antibodies against human and mouse ERK5, Phospho-ERK5 (Thr218/Tyr220), and IL-1β were obtained from Cell Signaling Technology. Anti-SYK antibody and anti-SYK (Phospho-Tyr525) antibody were purchased from Sangon Biotech. Anti-PYK2 antibody was obtained from Proteintech. Anti-PYK2 (Phospho-Tyr402) antibody and anti-BTK antibody were purchased from ABclonal. Anti-BTK (Phospho-Tyr223) antibody was purchased from Abcam.

Isolation of colon epithelial cells

The colons of mice were excised and washed with cold PBS and then cut into mini sections. The mini sections were incubated with Hanks-balanced salt solution containing 1 mM DTT, 5 mM EDTA, and 1% penicillin/streptomycin at 37 °C for 30 min with gentle shaking. The supernatant was filtered through a 100-μm cell strainer to remove any cell clumps and centrifuged. The cells were resuspended and cultured in DMEM containing 10% FBS and 1% penicillin/streptomycin.

Cell culture and stimulation

For BMDMs, bone marrow cells were collected from tibias and femurs by flushing with DMEM containing 10% FBS and 1% penicillin/streptomycin. The cell suspension was filtered through a 40-μm cell strainer to remove any cell clumps and then the bone marrow cells were cultured in DMEM containing 10% FBS, 1% penicillin/streptomycin, and 20% L929 culture supernatant. For peritoneal macrophages (PEMs), mice were intraperitoneally injected with 2.5 ml 4% sterile thioglycollate medium; 3 days later, the mice were sacrificed and the peritoneal cavities were washed with 5 ml PBS twice, then the cell suspension was filtered through a 70-μm cell strainer to remove any cell clumps. PEMs were then cultured in DMEM containing 10% FBS and 1% penicillin/streptomycin. HEK293T cells were cultured in DMEM containing 10% FBS and 1% penicillin/streptomycin. For NLRP3 inflammasome activation, macrophages were seeded in 12-well plates (1×10^6 cells per well) overnight, the cells were primed with LPS (500 ng/ml) for 6 h and then stimulated with 5 mM ADP (1 h), 5 mM ATP (1 h), 200 μg/ml MSU (4 h), and 500 μg/ml ALUM (4 h). After stimulation, cell lysates and supernatants were collected and analyzed by western blot or ELISA.

ADP release assay

Eight-week-old mice were treated with water containing 2.5% DSS for 7 days, then the mice were sacrificed and the colons were excised. The colons were then cut into mini sections and 0.15 g

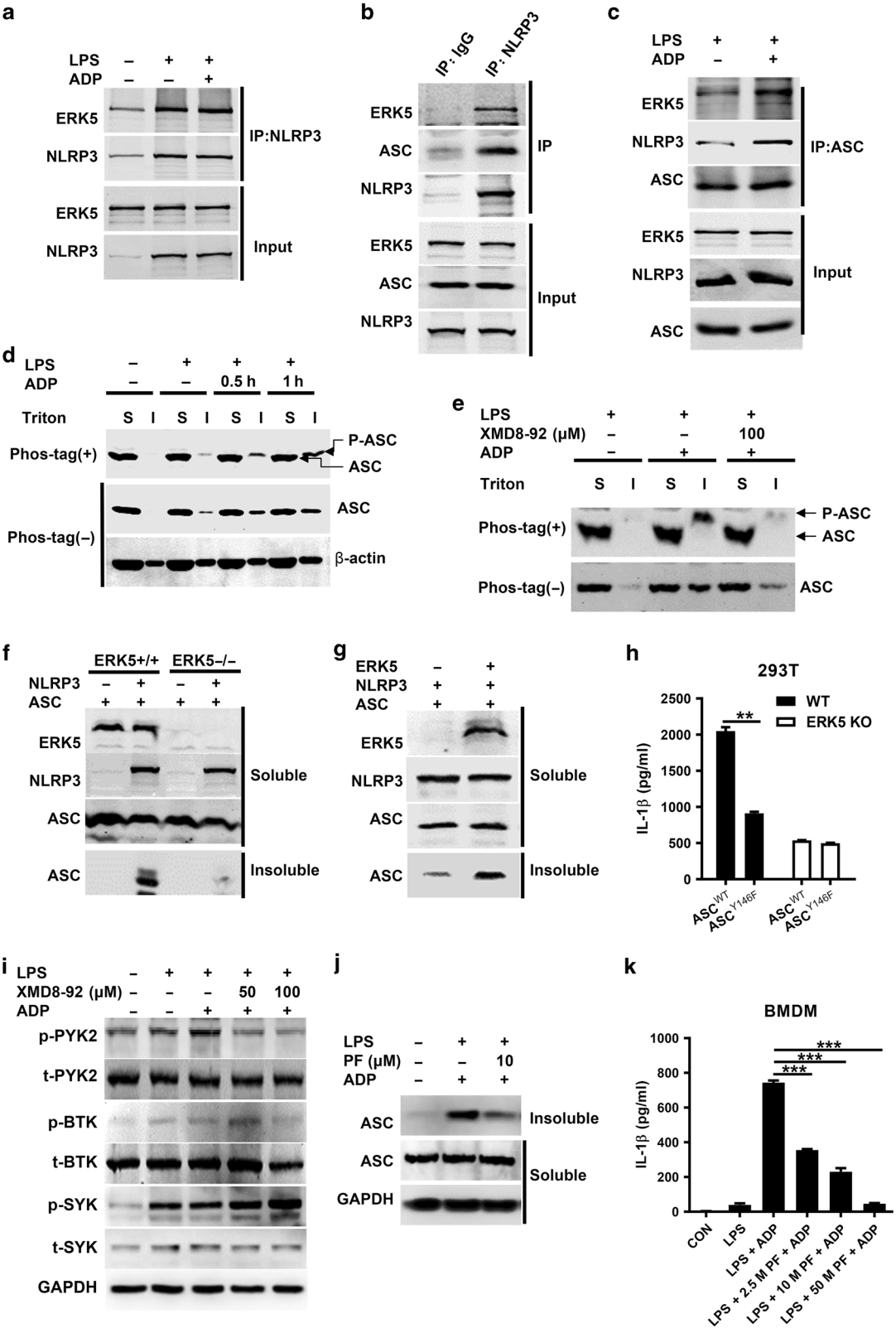

colon fractions were cultured in 24-well-plates (500 µl DMEM containing 10% FBS and 1% penicillin/streptomycin) for 6 h. ADP release in the supernatant was detected using the ADP-Glo™ Kinase Assay Kit according to the manufacturer's protocol.

ELISA

Supernatants from cell or tissue culture, serum, and peritoneal lavage fluids were collected. Levels of mouse IL-1β (BD Biosciences), IL-18 (eBioscience), TNF-α (BioLegend), IL-6

Fig. 7 ERK5 interacts with NLRP3/ASC and regulates ASC phosphorylation. a LPS-primed BMDM cells were stimulated with ADP (5 mM) or not for 1 h, then the ERK5-NLRP3 interaction was assessed by immunoprecipitation and immunoblotting. **b** LPS-primed BMDM cells were stimulated with ADP (5 mM) for 1 h, and the ERK5-NLRP3-ASC interaction was assessed by immunoprecipitation and immunoblotting. **c** LPS-primed BMDM cells were stimulated with ADP (5 mM) or not for 1 h, then the ERK5-NLRP3-ASC interaction was assessed by immunoprecipitation and immunoblotting. **d** LPS-primed BMDM cells were stimulated with ADP (5 mM) or not for the indicated times. Phosphorylated and total ASC in Triton X-soluble and Triton X-insoluble fractions were analyzed by SDS-PAGE with (+) or without (−) Phos-tag. **e** LPS-primed BMDM cells were pretreated with XMD8-92 (100 μM) or not for 1 h and then stimulated with ADP (5 mM) for 1 h. Phosphorylated and total ASC in Triton X-soluble and Triton X-insoluble fractions were analyzed by SDS-PAGE with (+) or without (−) Phos-tag. **f** The NLRP3 inflammasome was reconstituted in ERK5$^{+/+}$ and ERK5$^{-/-}$ 293T cells by transfection of GFP-NLRP3 and Myc-ASC for 30 h, and ASC in the Triton X-soluble (top three blots) and Triton X-insoluble (bottom blot) fractions was analyzed by immunoblotting. **g** The NLRP3 inflammasome was reconstituted in ERK5$^{-/-}$ 293T cells by transfection of HA-ERK5, GFP-NLRP3, and Myc-ASC for 30 h. ASC in Triton X-soluble and Triton X-insoluble fractions was analyzed by immunoblotting. **h** The NLRP3 inflammasome was reconstituted in ERK5$^{+/+}$ and ERK5$^{-/-}$ 293T cells by transfection of GFP-NLRP3, Myc-ASC^{WT} or Myc-ASC^{Y146F}, Myc-Pro-caspase-1, and Pro-IL-1β for 48 h. **i** LPS-primed BMDM cells were pretreated with 50 or 100 μM XMD8-92 for 1 h and then stimulated with ADP (5 mM) for 1 h. The phosphorylation of SYK, PYK2, and BTK were analyzed by immunoblotting. **j** LPS-primed BMDM cells were pretreated with PF-431396 (10 μM) or not for 1 h and then stimulated with ADP (5 mM) for 1 h. ASC in Triton X-soluble and Triton X-insoluble fractions was analyzed by immunoblotting. **k** LPS-primed BMDM cells were pretreated with indicated concentrations of PF-431396 for 1 h and then stimulated with ADP (5 mM) for 1 h. Production of IL-1β was detected by ELISA. Data are shown as mean ± SEM. $^{**}p < 0.01$; $^{***}p < 0.001$.

(BioLegend), and human IL-1β (BioLegend) were measured by ELISA according to the manufacturer's instructions.

siRNA

BMDMs or PEMs were plated in 12-well plates overnight and then transfected with 100 nM siRNA (GenePharma) using Lipofectamine 2000 (Invitrogen) according to the manufacturer's instructions. The siRNA sequences were: negative control, sense, 5′-UUCUCC GAACGUGUCACGUTT-3′, antisense, 5′-ACGUGACACGUUCGG AGA-ATT-3′; siERK5-1, sense, 5′-CCCUGGAACAUGUGAGAUATT-3′, anti-sense:5′-U AUCUCACAUGUUCCAGGGTT-3′; siERK5-2, sense:5′-GAC GCAUGUUGCGAUUUG ATT-3′, antisense:5′-UCAAAUCGCAACAUG CGUCTT-3′. siGαq-1, sense:5′-GAAGG UGUCUGCUUUUGAGTT-3′, antisense:5′-CUCAAAAGCAGACACCUUCTT-3′; si Gαq-2, sense:5′-GGAGUACAAUCUGGUCUAATT-3′, antisense:5′-UUAGACCAGAU U GUACUCCTT-3′.

Plasmids

GFP-NLRP3 (73955), Myc-ASC (73952), Myc-Pro-caspase-1 (41552), and HA-ERK5 (53175) were obtained from Addgene. Flag-tagged human Pro-IL-1β was amplified from LPS-primed BMDM cDNA and cloned into pcDNA3.1 plasmid. The sequence-specific primers carrying BamH I and Xho I restriction enzyme sites were: sense, 5′-CGGGATCCATGGCAGAAGTACCTGAG-3′, antisense:5′- CCGCTCG AGT TACGAAGACACAAATTG-3′. Flag-tagged human ERK5-ΔKD was amplified from HA-ERK5 (53175); the sequence-specific primers carrying BamH I and Xho I restriction enzyme sites were: sense, 5′-CGGGATCCCCTGGCTGTCCAGATGTT-3′, antisense:5′-CCG CTCGAGTCAGGGGTCCTGGAGGTC-3′. Myc-ASC^{Y146F} was amplified from Myc-ASC (73952), the sequence-specific primers were: sense: 5′-GAC GGATGAGCAGTTCCAGGCAGTGCGGGC-3′, antisense: 5′-GCCCGCACTGCCTG GAACTGCTCATCCGTC-3′.

LPS-induced endotoxic shock model

Eight-week-old mice were intraperitoneally injected with 20 mg/kg LPS for 6 h and then intraperitoneally injected with 300 mg/kg ADP for 1 h or LPS plus XMD8-92 for 6 h. The serum and peritoneal lavage fluids (500 μl PBS wash of the peritoneal cavities) were collected and the cytokines were measured by ELISA.

DSS-induced colitis, clinical scoring, and histopathological analysis

Colitis was induced in mice by administration of water containing 2 or 2.5% DSS for the indicated number of days. The DAI was the sum of weight loss, stool consistency, and rectal bleeding and monitored every day. Briefly, loss of body weight (0, no weight loss; 1, 1–5% weight loss; 2, 5–10% weight loss; 3, 10–20% weight loss; 4, >20% weight loss), stool consistency (0, normal stool; 2, loose stool; 4, diarrhea), and rectal bleeding (0, normal; 2, positive fecal occult blood test; 4, gross rectal bleeding). For histopathological analysis, colon tissues were fixed with 4% paraformaldehyde in PBS overnight and embedded into paraffin, then the tissue was cut into 6 μm slices and stained with hematoxylin/eosin solution (H&E). Histological score of colonic injury was evaluated based on the extent of inflammatory infiltration, loss of crypt, and tissue damage. Briefly, the inflammatory infiltration score was defined as follows: 0, no infiltrate; 1, mild infiltrate; 2, moderate infiltrate; and 3, severe infiltrate. Loss of crypt score was defined as follows: 0, no crypt loss; 1, 1–25% crypt loss; 2, 26–50% crypt loss; 3, 51–75% crypt loss; and 4, 76–100% crypt damage. Tissue damage included mucosal ulceration and depth of injury. Mucosal ulceration was defined as follows: 0, no ulcers; 1, focal ulcers; 2, multifocal ulcers; and 3, diffuse ulcers. The depth of injury was defined as follows: 0, no injury; 1, mucosal involvement only; 2, mucosal and submucosal involvement; and 3, transmural involvement.

Quantitative real-time PCR (Q-PCR)

BMDMs were lysed in RNAiso plus (TaKaRa) and cDNA was synthesized from extracted total RNA using the Prime Script RT Master Mix Perfect Real Time kit (TaKaRa) according to the manufacturer's protocol. Q-PCR was performed using SYBR Green premix (TaKaRa) and 500 ng cDNA was used as a template. β-actin was used as an internal control gene. The sequence-specific primers are listed in Supplementary Table 1.

Immunofluorescence

LPS-primed BMDMs were treated with XMD8-92 for 1 h and then stimulated with ADP (5 mM) for 1 h. The cells were then fixed with 4% PFA in PBS for 15 min and permeabilized with 0.1% Triton X-100 for 10 min. After blocking with 5% BSA in PBS, cells were incubated with an anti-ASC antibody overnight and then stained with Alexa Fluor 488-conjugated secondary Ab. After staining nuclei with DAPI, stained cells were visualized using a fluorescence microscope.

Immunoblot analysis

After stimulation, cells were lysed in SDS loading buffer and supernatants were concentrated. The samples were separated by 12% SDS-PAGE, transferred to nitrocellulose membranes and blocked with 5% BSA. After hybridization with primary Abs and appropriate fluorophore-conjugated secondary Abs, protein bands were visualized with the Odyssey laser digital imaging system (Gene Company).

Immunoprecipitation

LPS-primed BMDMs were stimulated with ADP or held as controls and then resuspended in lysis buffer (50 mM Tris, pH 7.4, 150 mM

NaCl, 2 mM EDTA, 0.5% Nonidet P-40, EDTA-free protease inhibitor cocktail). Cell lysates were centrifuged and clarified by protein G Agarose. The precleared cell lysates were immunoprecipitated with anti-NLRP3 or anti-ASC antibodies at 4 °C overnight and then pulled down by protein G Agarose and assessed by immunoblotting.

Reconstitution of NLRP3 inflammasome in HEK293T cells
HEK293T cells were plated in 12-well plates (3×10^5 cells per well) overnight. The cells were then transfected with plasmids expressing GFP-NLRP3 (150 ng), Myc-ASC or Myc-ASC^{Y146F} (100 ng), Myc-pro-caspase-1 (50 ng), and pro-IL-1β (100 ng) using Lipofectamine 2000. After 36 h, cell supernatants were collected and the maturation of IL-1β was measured by ELISA.

Phosphorylated ASC detection
LPS-primed BMDMs were pretreated with XMD8-92 (100 μM) or not for 1 h and then stimulated with ADP (5 mM) for 1 h. The cells were lysed with lysis buffer (50 mM Tris-HCl, pH 7.6, 0.5% Triton X-100, EDTA-free protease inhibitor cocktail, phosphatase inhibitor cocktail) and centrifuged at $6000 \times g$ for 15 min at 4 °C. Supernatants were referred to as the Triton X-100-soluble fractions and the pellets were considered the Triton X-100-insoluble fractions. The Triton X-100-soluble fractions and Triton X-100-insoluble fractions were then analyzed by SDS-PAGE with (+) or without (−) Phos-tag acrylamide (Alpha Labs, AAL-107) (20 μM) and $MnCl_2$ (50 μM).

Generation of ERK5-knockout cell line
To generate an ERK5-knockout cell line, the CRISPR/Cas9 system was used. In brief, LentiCRISPRv2 plasmid containing the ERK5-knockout target sequence 5′-CAGGTTCTTGGCCGCTACAG-3′ was transduced into HEK293T cells. Three days later, puromycin-resistant single clones were selected and the ERK5-knockout clones were identified by western blot with an anti-ERK5 antibody.

Statistical analysis
All data were analysed using the GraphPad Prism software and expressed as the mean ± SEM. The Student's *t* test (two-tailed) was used to analyze the significance of data and p value < 0.05 was considered statistically significant.

DATA AVAILABILITY

All data that support the findings of this study are available from the corresponding authors upon request.

ACKNOWLEDGEMENTS

This work was supported by National Key R&D Program of China [2018YFA0507001 to B.D.]; National Natural Science Foundation of China [31770969 to B.D., 81672811 and 81871250 to M.Q., and 81830083 to M.L., 81902892 to J.Q.]; Innovation Program of Shanghai Municipal Education Commission [2017-01-07-00-05-E00011 to M.L.]; and Natural Science Foundation of Jiangsu Province [Grant no. BK20190657 to C.Z.].

AUTHOR CONTRIBUTIONS

B.D., M.Q., and M.L. supervised the project. B.D. and C.Z. conceived and designed the experiments. C.Z., J.Q., S.Z., N.Z., Y.Z., and B.T. performed the experiments. B.D., C.Z., Q.W., S.S., and J.C. analyzed the data. B.D., S.S., and C.Z. wrote the manuscript.

ADDITIONAL INFORMATION

The online version of this article (https://doi.org/10.1038/s41385-020-0307-5) contains supplementary material, which is available to authorized users.

Competing interests: The authors declare no competing interests.

Publisher's note Springer Nature remains neutral with regard to jurisdictional claims in published maps and institutional affiliations.

REFERENCES

1. Guo, H., Callaway, J. B. & Ting, J. P. Inflammasomes: mechanism of action, role in disease, and therapeutics. *Nat. Med.* **21**, 677–687 (2015).
2. Vanaja, S. K., Rathinam, V. A. & Fitzgerald, K. A. Mechanisms of inflammasome activation: recent advances and novel insights. *Trends Cell Biol.* **25**, 308–315 (2015).
3. de Almeida, L. et al. The PYRIN domain-only protein POP1 inhibits inflammasome assembly and ameliorates inflammatory disease. *Immunity* **43**, 264–276 (2015).
4. Ungaro, R., Mehandru, S., Allen, P. B., Peyrin-Biroulet, L. & Colombel, J. F. Ulcerative colitis. *Lancet* **389**, 1756–1770 (2017).
5. Neurath, M. F. Cytokines in inflammatory bowel disease. *Nat. Rev. Immunol.* **14**, 329–342 (2014).
6. Xu, J. et al. The REGgamma-proteasome forms a regulatory circuit with Ikappaβvarepsilon and NFkappaB in experimental colitis. *Nat. Commun.* **7**, 10761 (2016).
7. Lynch, W. D. & Hsu, R. *Ulcerative Colitis*. (StatPearls, Treasure Island, FL, 2018).
8. Dinarello, C. A. Biologic basis for interleukin-1 in disease. *Blood* **87**, 2095–2147 (1996).
9. Coccia, M. et al. IL-1beta mediates chronic intestinal inflammation by promoting the accumulation of IL-17A secreting innate lymphoid cells and CD4(+) Th17 cells. *J. Exp. Med.* **209**, 1595–1609 (2012).
10. Bauer, C. et al. Colitis induced in mice with dextran sulfate sodium (DSS) is mediated by the NLRP3 inflammasome. *Gut* **59**, 1192–1199 (2010).
11. Seo, S. U. et al. Distinct commensals induce interleukin-1beta via NLRP3 inflammasome in inflammatory monocytes to promote intestinal inflammation in response to injury. *Immunity* **42**, 744–755 (2015).
12. Perera, A. P. et al. MCC950, a specific small molecule inhibitor of NLRP3 inflammasome attenuates colonic inflammation in spontaneous colitis mice. *Sci. Rep.* **8**, 8618 (2018).
13. Cosin-Roger, J. et al. Hypoxia ameliorates intestinal inflammation through NLRP3/mTOR downregulation and autophagy activation. *Nat. Commun.* **8**, 98 (2017).
14. Russo, M. V. & McGavern, D. B. Immune surveillance of the CNS following infection and injury. *Trends Immunol.* **36**, 637–650 (2015).
15. Eltzschig, H. K., Sitkovsky, M. V. & Robson, S. C. Purinergic signaling during inflammation. *N. Engl. J. Med.* **367**, 2322–2333 (2012).
16. Cho, J. et al. Purinergic P2Y(1)(4) receptor modulates stress-induced hematopoietic stem/progenitor cell senescence. *J. Clin. Investig.* **124**, 3159–3171 (2014).
17. Elliott, M. R. et al. Nucleotides released by apoptotic cells act as a find-me signal to promote phagocytic clearance. *Nature* **461**, 282–286 (2009).
18. Chen, Y. et al. Purinergic signaling: a fundamental mechanism in neutrophil activation. *Sci. Signal.* **3**, ra45 (2010).
19. Ghiringhelli, F. et al. Activation of the NLRP3 inflammasome in dendritic cells induces IL-1beta-dependent adaptive immunity against tumors. *Nat. Med.* **15**, 1170–1178 (2009).
20. Li, R. et al. Extracellular UDP and P2Y6 function as a danger signal to protect mice from vesicular stomatitis virus infection through an increase in IFN-beta production. *J. Immunol.* **193**, 4515–4526 (2014).
21. Zhang, X. et al. Extracellular ADP facilitates monocyte recruitment in bacterial infection via ERK signaling. *Cell Mol. Immunol.* **15**, 58–73 (2018).
22. Zhang, C. et al. IFN-stimulated P2Y13 protects mice from viral infection by suppressing the cAMP/EPAC1 signaling pathway. *J. Mol. Cell Biol.* **11**, 395–407 (2019).
23. Jacobson, K. A. et al. Nucleotides acting at P2Y receptors: connecting structure and function. *Mol. Pharmacol.* **88**, 220–230 (2015).
24. Zhang, D. et al. Two disparate ligand-binding sites in the human P2Y1 receptor. *Nature* **520**, 317–321 (2015).
25. Wujak, M., Hetmann, A., Porowinska, D. & Roszek, K. Gene expression and activity profiling reveal a significant contribution of exo-phosphotransferases to the extracellular nucleotides metabolism in HUVEC endothelial cells. *J. Cell Biochem.* **118**, 1341–1348 (2017).
26. Lee, G. S. et al. The calcium-sensing receptor regulates the NLRP3 inflammasome through Ca2+ and cAMP. *Nature* **492**, 123–127 (2012).
27. Natrajan, R. et al. Amplification and overexpression of CACNA1E correlates with relapse in favorable histology Wilms' tumors. *Clin. Cancer Res.* **12**, 7284–7293 (2006).
28. Sacchetti, P., Carpentier, R., Segard, P., Olive-Cren, C. & Lefebvre, P. Multiple signaling pathways regulate the transcriptional activity of the orphan nuclear receptor NURR1. *Nucleic Acids Res.* **34**, 5515–5527 (2006).
29. Nicol, R. L. et al. Activated MEK5 induces serial assembly of sarcomeres and eccentric cardiac hypertrophy. *EMBO J.* **20**, 2757–2767 (2001).
30. Mao, K. et al. Nitric oxide suppresses NLRP3 inflammasome activation and protects against LPS-induced septic shock. *Cell Res.* **23**, 201–212 (2013).
31. Baroja-Mazo, A. et al. The NLRP3 inflammasome is released as a particulate danger signal that amplifies the inflammatory response. *Nat. Immunol.* **15**, 738–748 (2014).

32. Hara, H. et al. Phosphorylation of the adaptor ASC acts as a molecular switch that controls the formation of speck-like aggregates and inflammasome activity. *Nat. Immunol*. **14**, 1247–1255 (2013).
33. Ito, M. et al. Bruton's tyrosine kinase is essential for NLRP3 inflammasome activation and contributes to ischaemic brain injury. *Nat. Commun*. **6**, 7360 (2015).
34. Chung, I. C. et al. Pyk2 activates the NLRP3 inflammasome by directly phosphorylating ASC and contributes to inflammasome-dependent peritonitis. *Sci. Rep*. **6**, 36214 (2016).
35. Ranson, N., Kunde, D. & Eri, R. Regulation and sensing of inflammasomes and their impact on intestinal health. *Int. J. Mol. Sci*. **18**, 2379 (2017).
36. Kurashima, Y. et al. Extracellular ATP mediates mast cell-dependent intestinal inflammation through P2X7 purinoceptors. *Nat. Commun*. **3**, 1034 (2012).
37. Ali, S. R. et al. Anthrax toxin induces macrophage death by p38 MAPK inhibition but leads to inflammasome activation via ATP leakage. *Immunity* **35**, 34–44 (2011).
38. Tang, T., Gong, T., Jiang, W. & Zhou, R. GPCRs in NLRP3 inflammasome activation, regulation, and therapeutics. *Trends Pharm. Sci*. **39**, 798–811 (2018).
39. Heredia, D. J. & Feng, C. Y. Activity-induced Ca(2+) signaling in perisynaptic Schwann cells of the early postnatal mouse is mediated by P2Y1 receptors and regulates muscle fatigue. *Elife*. **7**, e30839 (2018).
40. Mega, J. L. & Simon, T. Pharmacology of antithrombotic drugs: an assessment of oral antiplatelet and anticoagulant treatments. *Lancet* **386**, 281–291 (2015).
41. Murakami, T. et al. Critical role for calcium mobilization in activation of the NLRP3 inflammasome. *Proc. Natl Acad. Sci. USA* **109**, 11282–11287 (2012).
42. Yan, Y. et al. Dopamine controls systemic inflammation through inhibition of NLRP3 inflammasome. *Cell* **160**, 62–73 (2015).
43. Levesque, S. A., Kukulski, F., Enjyoji, K., Robson, S. C. & Sevigny, J. NTPDase1 governs P2X7-dependent functions in murine macrophages. *Eur. J. Immunol*. **40**, 1473–1485 (2010).
44. Cohen, H. B. et al. TLR stimulation initiates a CD39-based autoregulatory mechanism that limits macrophage inflammatory responses. *Blood* **122**, 1935–1945 (2013).
45. Jorgensen, I. & Miao, E. A. Pyroptotic cell death defends against intracellular pathogens. *Immunol. Rev*. **265**, 130–142 (2015).
46. Rossol, M. et al. Extracellular Ca2+ is a danger signal activating the NLRP3 inflammasome through G protein-coupled calcium sensing receptors. *Nat. Commun*. **3**, 1329 (2012).
47. Latz, E., Xiao, T. S. & Stutz, A. Activation and regulation of the inflammasomes. *Nat. Rev. Immunol*. **13**, 397–411 (2013).
48. Zhou, G., Bao, Z. Q. & Dixon, J. E. Components of a new human protein kinase signal transduction pathway. *J. Biol. Chem*. **270**, 12665–12669 (1995).
49. Kipniss, N. H., Dingal, P. & Abbott T. R. Engineering cell sensing and responses using a GPCR-coupled CRISPR-Cas system. *Nat. Commun*. **8**, 2212 (2017).
50. Guo, C. et al. Bile acids control inflammation and metabolic disorder through inhibition of NLRP3 inflammasome. *Immunity* **45**, 802–816 (2016).
51. Zhang, C. et al. Virus-triggered ATP release limits viral replication through facilitating IFN-beta production in a P2X7-dependent manner. *J. Immunol*. **199**, 1372–1381 (2017).
52. Andre, P. et al. P2Y12 regulates platelet adhesion/activation, thrombus growth, and thrombus stability in injured arteries. *J. Clin. Investig*. **112**, 398–406 (2003).